Co-published by
Institute of Fluid-Flow Machinery
Polish Academy of Sciences
Committee on Thermodynamics and Combustion
Polish Academy of Sciences

http://www.imp.gda.pl/archives-of-thermodynamics/

Influence of vortex generator dimensions on film cooling efficiency

Mohammed Larbi[a], Khadidja Boualem[b*], Siham Kerrouz[b], Fatima Benali Kouchih[a], Tayeb Yahiaoui[a], Abbes Azzi[a]

[a]University of Sciences and Technology of Oran - Mohammed Boudiaf, P.O. Box 1505, El-M'Naouer, 31000, Oran, Algeria
[b]University of Relizane, Algeria
*Corresponding author email: khadidja.boualem@univ-relizane.dz

Received: 06.01.2024; revised: 13.09.2024; accepted: 29.10.2024

Abstract

Enhancements in gas turbine blade cooling techniques, such as film cooling, have significantly advanced the aerothermal efficiency of turbines, especially in transportation sectors like aeronautics and automotive industries. This study aims to enhance turbine blade cooling by incorporating an obstruction at the jet exit. The vortex generator angle has been modified to 25°, 45°, 60°, 90° and 110°. These five designs were assessed in comparison to the conventional cylindrical hole configurations. Two injection ratios (M = 0.25, and M = 0.5) were studied within the ANSYS CFX 16 software, utilizing the finite volume method to solve the average Reynolds equations and the energy equation. The findings show qualitative alignment with experimental data for the base scenario, indicating that the vortex generator angle notably amplifies film cooling effectiveness. Typically, the vortex generator configured at 90° exhibits a stronger mixing capability compared to the other cases and cylindrical design.

Keywords: Film cooling efficiency; Vortex generator angle; Vortex structures; Area weighted film cooling

Vol. 45(2024), No. 4, 197–203; doi: 10.24425/ather.2024.152009

Cite this manuscript as: Larbi, M., Boualem, K., Kerrouz, S., Benali Kouchih, F., Yahiaoui, T., & Azzi, A. (2024). Influence of vortex generator dimensions on film cooling efficiency. *Archives of Thermodynamics*, 45(4), 197−203.

1. Introduction

Gas turbine blade cooling techniques such as film cooling have helped improve the aerothermal efficiency of turbines. Film cooling stands out as the predominant and most efficient system employed in the industry to cool gas turbine blades. Pioneering studies in film cooling, especially exploring advancements in film geometries were initiated by the work of Goldstein [1]. The film cooling efficiency and the heat transfer coefficients were experimentally established by Liess [2], accounting for the impact of blowing ratios and Mach numbers. Paradis [3] demonstrated the effects of blowing rates and temperature variations on the efficiency of film cooling. The findings reported in the work of Jabbari and Goldstein [4] demonstrate that, at unity, the blowing ratio causes the heat transfer coefficient to increase.

The most common disadvantage of film cooling system is that the flow rises from the surface in the form of two vortices. Counter-current vortices introduce hot air into the jet and destroy the protective film of cold air. Several shapes have been used to improve the cooling performance. Azzi and Jubran [5] conducted a numerical study of a configuration console for controlling the intensity of counter-rotating vortex pairs (CRVP). It was demonstrated that the two counter-rotating vortices that cause the protective coating to deteriorate are absent from the flow structure provided by the new geometry. According to Khorsi and Azzi [6], the converging slot hole (console) provides greater efficiency than the traditional cylinder hole in the same situation. According to Guangchao et al.'s research [7], raising the momentum flux ratio for the injection through fanned holes causes the heat transfer to decrease and the effectiveness of film

Nomenclature

c_p – specific heat at constant pressure, J/(kg K)
D – film-cooling hole diameter, mm
k – turbulent kinetic energy, m^2/s^2
L – spanwise dimension of the flat plate, mm
M – blowing ratio
P_k – production term, W
T – temperature, K
Tu – turbulence intensity, %
u_i – velocity components, m/s
x, y, z – Cartesian coordinates, m

Greek symbols

$\delta_{i,j}$ – unit tensor components
ε – dissipation rate of turbulent kinetic energy, m^2/s^3
η – adiabatic film cooling efficiency
λ – thermal conductivity, W/(m K)
μ – dynamic viscosity, Pa·s
μ_t – turbulent dynamic viscosity, Pa s
ρ – density, kg/m^3

Subscripts and Superscripts

c – cooling
i, j – indexes
w – wall (flat plate)
∞ – freestream condition

Abbreviations and Acronyms

CRVP – counter-rotating vortex pair
VG – vortex generator

cooling to increase dramatically. Liu et al. [8] measured the waist-shaped slot hole's film cooling performance and compared it to two different kinds of console holes. Console holes with a narrow area ratio provided the best thermal protection. Moreover, Zaman et al. [9] conducted experimental research on the flow structure of an inclined jet interacting with a vortex generator to enhance film-cooling techniques. Their work contributes significantly to advancing our understanding of film cooling mechanisms. The film cooling performance and flow characteristics of backward injection with combined holes is the focus of the investigations of Ben Ali Kouchih et al. [10].The findings suggest that backward injection achieves a uniform coverage, resulting in optimal cooling performance. Specifically, the most significant enhancement in film cooling is observed with the employment of combined holes in backward injection, especially at a blowing ratio of 1.5. The studies conducted by Boualem and Azzi [11] and Boualem and al. [12] focused on assessing the efficacy of cooling holes embedded within various trench designs. The primary finding indicates that utilizing jets installed within trenches significantly improves film cooling effectiveness, particularly at elevated blowing ratios.

Na and Shih [13] positioned a ramp preceding a coolant orifice to either eliminate or diminish the counter-rotating vortex pair (CRVP). Their findings showcase that managing the size of this counter-rotating vortex pair significantly enhances the cooling performance. Additionally, Zaman et al. [9] and Shinn et al. [14] have illustrated the film cooling distributions behind micro-ramps. These structures generate anti-vortices, effectively delaying the lifting-off of the jet. An et al. [15] carried out an experiment to investigate how the cooling performance was affected by a short crescent-shaped block positioned downstream of a cylindrical cooling hole. The results showed that this cresent-shaped block increases the lateral averaged film cooling when it is present. Meanwhile, Zhou and Hu [16,17] introduced a ramp design inspired by Barchan sand dunes. Their innovation significantly affects the Counter-Rotating Vortex Pair (CRVP), enhancing film cooling efficiency while minimizing aerodynamic losses. Grine et al. [18] combined two anti-vortex systems to enhance the film cooling efficiency. Ben Ali Kouchih et al. [19] investigated the effect of Barchan sand dunes on forward and backward injection hole. Their findings reportedly show a substantial enhancement in area-weighted film cooling.

The focus of many researchers revolves around altering the film hole shape at high ejection ratios to optimize film cooling efficiency. This paper specifically evaluates and compares the efficacy of a cylindrical hole placed within a vortex generator (VG) at low and medium blowing ratios against conventional cylindrical holes for enhancing film cooling efficiency without resorting to an increase in blowing. The assessment delves into the impact of various angle scales constituting the VG shape, including angles of 25°, 45°, 60°, 90° and 110°. These five configurations are tested across two blowing ratios 0.25 and 0.5 to comprehensively understand their performance under varying conditions.

2. Computational model and grid sensitivity study

Figure 1a presents the physical domain under consideration. The chosen base case aligns with Sinha et al.'s study [20], featuring hole dimensions of D = 1.27 cm and a length-to-diameter ratio of L/D = 1.75. The jet hole is inclined at a 35° angle to the flow direction. Within the computational space, dimensions span 20 times the diameter in height and 50 times the diameter in length.

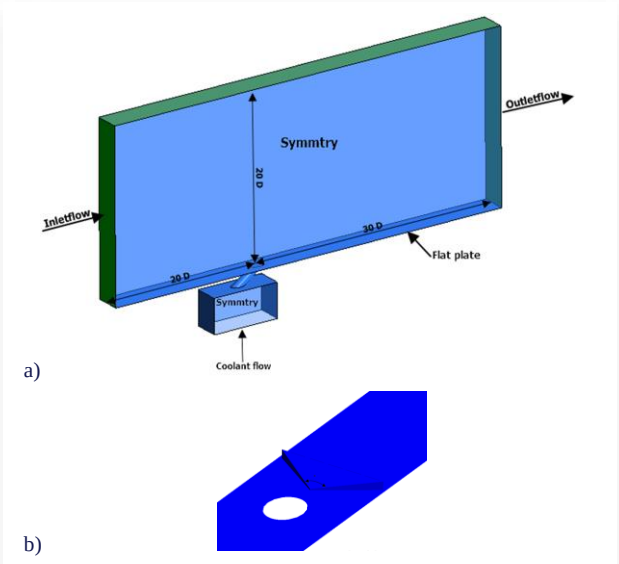

Fig. 1. a) Computational domain and boundary conditions; b) Vortex generator design.

The novel design proposed in this paper is to install a vortex generator at the outlet jet by changing the angle of the vertex of the triangle to 25°, 45°, 60°, 90° and 110° as presented in Fig. 1b. Two injection ratios $M = \rho_c U_c/(\rho_\infty U_\infty) = 0.25$ and 0.5 were investigated. The ratio ρ_c/ρ_∞ is fixed to 1.2. The methods used should be general, allowing one to solve a similar class of problems. The boundary conditions are presented in Table 1.

Table 1. Boundary conditions.

Factor	Velocity [m/s]	Temperature [K]
Hot flow inlet	20	300
Cold flow inlet	$(MU_\infty\rho_\infty)/\rho_\infty$	250

The most important parameter in this topic is the adiabatic film cooling efficiency, which is defined by the following expression:

$$\eta = \frac{T_\infty - T_W}{T_\infty - T_c}. \quad (1)$$

2.1. Turbulence modelling

To carry out this work, several simulations were conducted using ANSYS CFX 14.0 software. In the solver package, the solution of the Reynolds averaged Navier–Stokes equations (RANS) is obtained by using the finite volume method for discretization of the continuity, momentum and energy equations. The second-order upwind solution scheme is used to solve the momentum, energy and turbulence model equations. The SIMPLEC algorithm is employed to solve the pressure–velocity coupling. The governing equations that include the conservation of mass, momentum and energy can be written as follows:

$$\frac{\partial(\rho u_i)}{\partial x_i} = 0, \quad (2)$$

$$\rho\bar{u}_j\frac{\partial\bar{u}_i}{\partial x_j} = -\frac{\partial\bar{p}}{\partial x_i} + \frac{\partial}{\partial x_j}\left[\mu\left(\frac{\partial\bar{u}_i}{\partial x_j} + \frac{\partial\bar{u}_j}{\partial x_i}\right) - \overline{\rho u_i' u_j'}\right], \quad (3)$$

$$\frac{\partial}{\partial x_i}(\rho u_i T) = \frac{\partial}{\partial x_j}\left[\left(\frac{\lambda}{C_p} + \frac{\mu_t}{Pr_t}\right)\frac{\partial T}{\partial x_j}\right], \quad (4)$$

where μ_t and Pr_t are the turbulent viscosity and turbulent Prandtl number, respectively.

Modelling of the Reynolds stresses $\left(-\rho\overline{u_i'u_j'}\right)$ in Eq. (3) is done using the Boussinesq hypothesis which relates the Reynolds stresses to the mean velocity gradients via Eq. (5) below:

$$-\rho\overline{u_i'u_j'} = \mu_t\left(\frac{\partial u_i}{\partial x_j} + \frac{\partial u_j}{\partial x_i}\right) - \frac{2}{3}\left(\rho k + \mu_t\frac{\partial u_i}{\partial x_i}\right)\delta_{ij}. \quad (5)$$

Turbulent quantities in the Navier–Stokes equations are treated using the turbulent viscosity μ_t given by:

$$\mu_t = \rho C_\mu\frac{k^2}{\varepsilon}, \qquad C_\mu = 0.085.$$

According to the literature survey, the RNG k–ε model is more consistent with the experimental data for the prediction of film cooling effectiveness than other models. This model has been adopted in our work. A detailed explanation of the model formulation and test case validations can be found in specific literature, whereas only the mathematical equations of the model are presented here:

$$\frac{\partial}{\partial t}(\rho k) + \frac{\partial}{\partial x_i}(\rho k u_i) = \frac{\partial}{\partial x_j}\left[\left(\mu + \frac{\mu_t}{\sigma_k}\right)\frac{\partial k}{\partial x_j}\right] + P_k - \rho\varepsilon, \quad (6)$$

$$\frac{\partial}{\partial t}(\rho\varepsilon) + \frac{\partial}{\partial x_i}(\rho\varepsilon u_i) = \frac{\partial}{\partial x_j}\left[\left(\mu + \frac{\mu_t}{\sigma_\varepsilon}\right)\frac{\partial\varepsilon}{\partial x_j}\right] + C_{1\varepsilon}\frac{\varepsilon}{k}P_k - C_{2\varepsilon}^*\rho\frac{\varepsilon^2}{k}, \quad (7)$$

where:

$$C_{2\varepsilon}^* = C_{2\varepsilon} + \frac{C_\mu\eta^3(1-\eta/\eta_0)}{1+\beta\eta^3},$$

$$\eta = Sk/\varepsilon, \qquad S = \left(2S_{ij}S_{ij}\right)^{1/2}.$$

The constants of the RNG k–ε model are mentioned in Table 2.

Table 2. Constants of the turbulence model.

C_μ	σ_k	σ_ε	$C_{1\varepsilon}$	$C_{2\varepsilon}$	η_0	β
0.0845	0.7194	0.7149	1.42	1.68	4.38	0.012

2.2. Mesh generation

In this study, geometry generation and mesh generation were performed using ICEM. The ANSYS CFX solver was used to solve the momentum equation, energy equation, and turbulence equation. The RNG k–ε model was used in this study. The ability of this model to predict film-cooling properties has been demonstrated by [21] and [22].

In the present investigation, the lowest freestream turbulence was chosen according to the work of Mayhew, who showed that at low blowing ratio the coverage area is reduced due to increased mixing with the main flow.

Validity of the calculation is ensured by comparing the results obtained in this study with the experimental data presented by [20], taking into account the sensitivity of the mesh. Three meshes are investigated: 1000000 nodes (coarse), 1500000 nodes (fine), and 2000000 nodes (very fine). The fine mesh adjustment is near the outlet jet area. Figure 2 shows the zoom area of a multi-block hexahedral mesh.

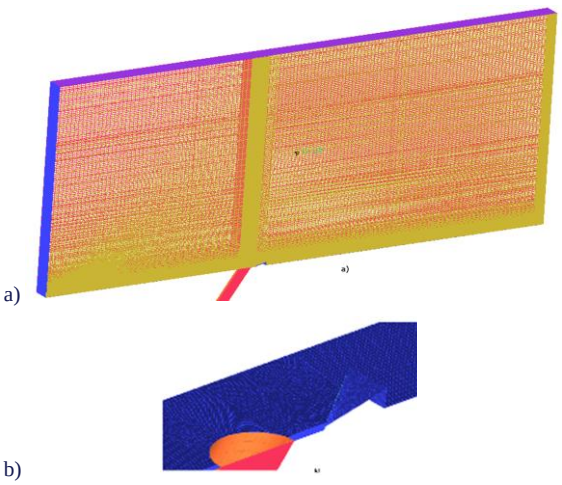

Fig. 2. a) Calculation grid, b) zoomed area of VG mesh.

Figure 3 shows the grid independence for a blowing ratio of M = 0.5. According to Fig. 4, the fine and very fine meshes give somewhat the same adiabatic film cooling in the flow direction, in contrast to the coarse mesh, which is less accurate, especially far from the jet hole. Since increasing the mesh nodes to 2 million does not make a significant difference, a fine mesh (1.5 million) was chosen and implemented in other configurations.

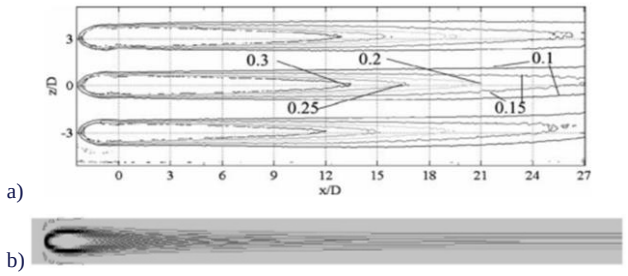

Fig. 3. Comparison of cooling efficiency contours, M = 0.5, Tu = 0.1%: a) Mayhew et al. [23], b) present investigation.

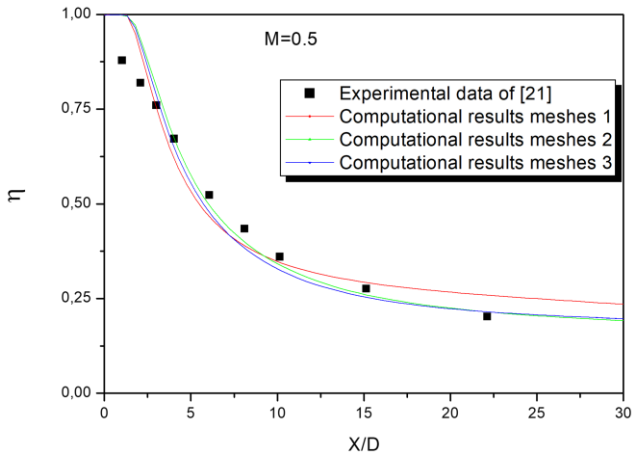

Fig. 4. Centreline adiabatic film cooling effectiveness for three different meshing.

The results indicate that the traditional film cooling design exhibits the lowest efficiency, while the new configurations demonstrate a substantially higher film cooling efficiency at both blowing ratios, 0.25 and 0.5. In some instances, the improvement rate exceeds 100%, emphasizing the significant enhancement achieved by employing these novel configurations with vortex generators in comparison to the conventional approach.

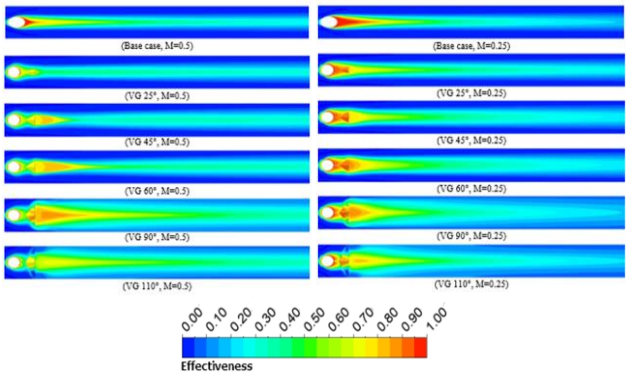

Fig. 5. Contours of adiabatic film cooling efficiency on the flat plate.

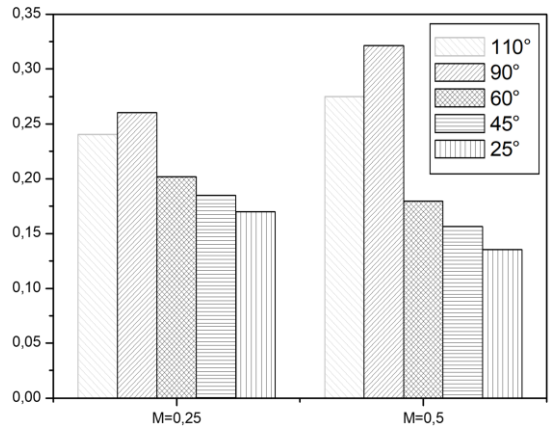

Fig. 6. Area weighted average film cooling efficiency.

3. Results and discussion

3.1. Film cooling efficiency

In Fig. 5, a comparison between the adiabatic cooling efficiency distributions on the flat plate is presented for the baseline case against the novel designs proposed in this study, particularly at low and medium blowing ratios (M = 0.25 and 0.5). The baseline case exhibits uneven coolant distribution due to jet lift-off, affecting the surface coverage. In contrast, the new designs, specifically with the degree of vortex generator configurations at 90° and 110° angles showcase notably improved film cooling efficiency distributions. This enhancement is attributed to the ability of the vortex generators to shape the coolant flow, ensuring more even distribution across the flat plate surface.

Figure 6 illustrates a quantitative assessment comparing the area-weighted average film cooling efficiency between two scenarios: the traditional case (flat plate without vortex generators) and the novel configurations (flat plate with vortex generators).

Figure 7 demonstrates the variation in film cooling efficiency for the two blowing ratios (0.25 and 0.5) across the twelve cases, including five new configurations alongside the baseline case. Notably, it is evident that the maximum efficiency occurs behind the film hole and decreases as the distance from the hole (x/D) increases across all configurations.

In the baseline cases, the cooling efficiency diminishes with increasing blowing ratios, which can be attributed to the jet take-off. However, with the incorporation of vortex generators (VGs), there is a substantial improvement in film cooling performance compared to the reference case.

Comparing the different angles of vortex generators with the traditional cylindrical hole case, it is observed that VG with a right angle generally delivers superior efficiency, except at M = 0.25, where there is a slight difference after x/D > 10, favouring the accurate trench configuration. Notably, at both blowing ratios, VG set at 90° consistently achieves the highest film cooling efficiency among the configurations tested.

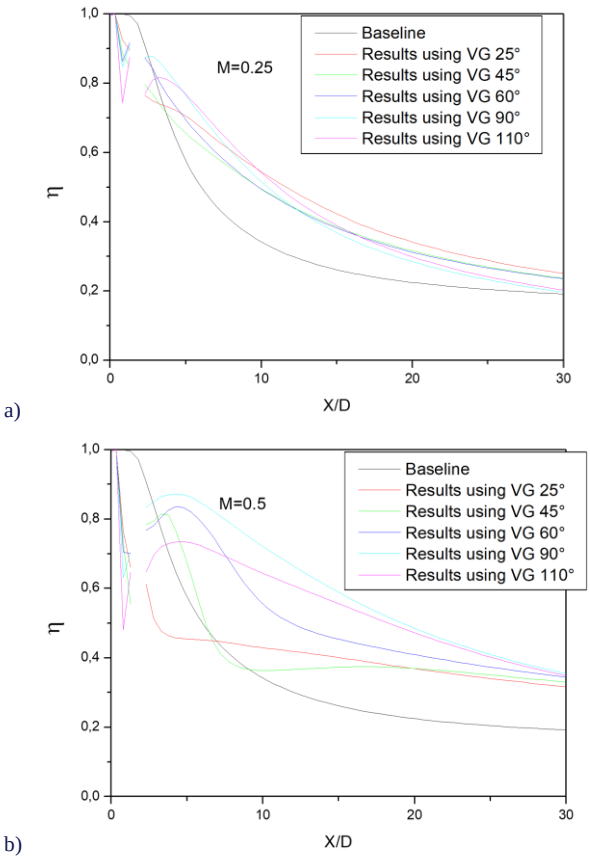

Fig. 7. Centreline adiabatic film cooling efficiency for all cases: a) M = 0.25, b) M = 0.5.

3.2. Flow structure

The formation of counter-rotating vortices (CRV), often termed kidney vortices, arises from the interaction between the mainstream and jet flows. These vortices significantly influence film-cooling performance, especially under high blowing ratios. Their passive nature involves reheating the air from the main flow, potentially compromising the protection provided to turbine blades or flat surfaces.

To gain deeper insights into the underlying physics and assess the impact of new designs on flow structures at blowing ratios of M = 0.25 and M = 0.5, Fig. 8 displays temperature contours in the y–z plane at x/D = 3, 6 and 10 for vortex generators with acute, right and obtuse angles. In the baseline case, higher injection rates lead to the jet moving away from the plate surface, enlarging the vortices. However, placing the vortex generator downstream of the jet outlet reduces the strength of the rotating vortices (CRV), encouraging the cooler flow to adhere more closely to the flat plate.

Figure 9 presents the vortex structures to better understand the flow behaviour. This figure shows that the distribution and efficiency of the cooling film are influenced by CRVP, horseshoes and shear layers. Due to the difference in momentum, the cooling jet can break away from the surface, creating a recirculation zone before reconnecting which we can observe from the baseline case. Notably, VGs with acute angles 25° exhibit lower efficiency in reducing CRVs compared to VGs with right and obtuse angles (90° and 110°), emphasizing the differential impact of VG angles on mitigating these detrimental vortices and enhancing film cooling performance.

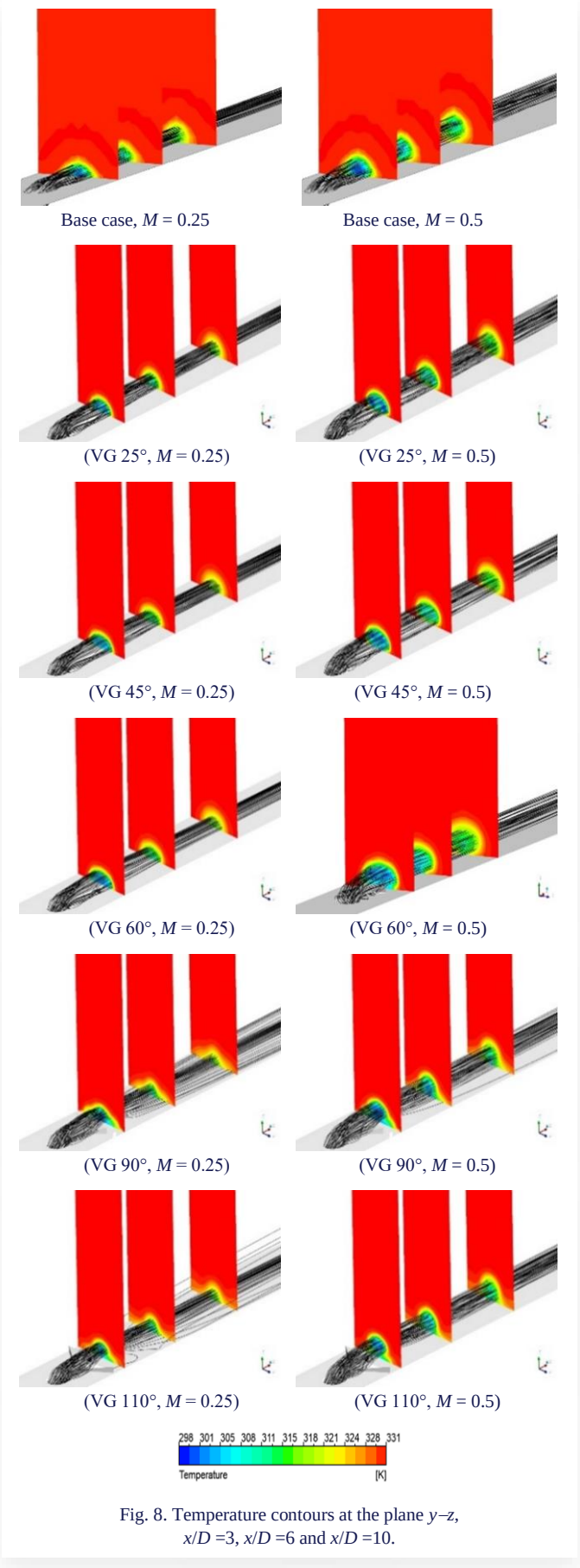

Fig. 8. Temperature contours at the plane y–z, x/D =3, x/D =6 and x/D =10.

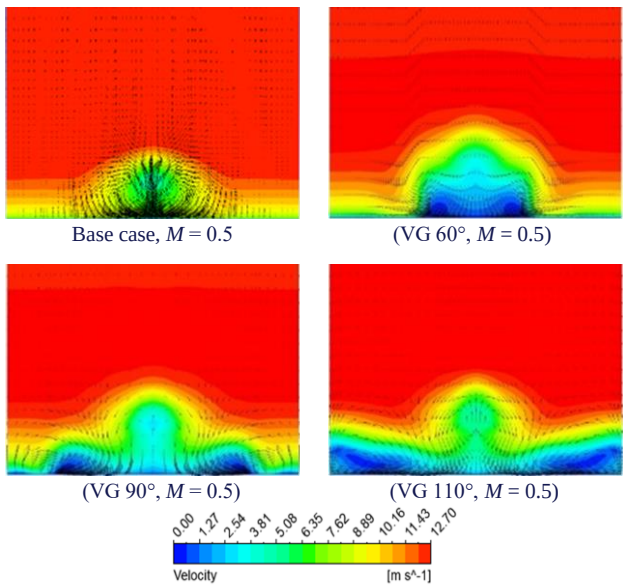

Fig. 9. Counter rotating vortex pairs at the plane $y–z$, x/D =3.

4. Conclusions

The numerical study focused on investigating the flow behaviour and thermal characteristics of film cooling across six different configurations. This analysis specifically considered the variation in the blowing ratio parameter, examining scenarios at M = 0.25 and M = 0.5. By exploring these different configurations and varying blowing ratios, the study aimed to understand in a comprehensive manner how changes in parameters affect flow patterns and thermal attributes, providing valuable insights into optimizing film cooling performance.

In the initial case, serving as the baseline for validation purposes, the efficiency of film cooling along the centreline was compared to the existing data. The results indicated that the computational model employed, based on the RNG $k–\varepsilon$ model, accurately predicted the flow structure and thermal behaviour in line with the available data. Moreover, an enhancement in film cooling performance was achieved by introducing vortex generators with 90° as an improvement over the original streamwise cylindrical injection method.

The main results from this work can be summarized as follows:

- the ability of vortex generators to distribute the coolant flow over the flat plate surface,
- the new configurations demonstrate significantly higher film cooling efficiency at both blowing ratios, 0.25 and 0.5, reaching or exceeding 100% in some cases,
- right or obtuse angle vortex generators help reduce the size of counter-rotating vortices, helping to distribute cool air.

References

[1] Goldstein, R.J. (1971). Film cooling. *Advances in heat transfer*, 7, 321–379. doi: 10.1016/S0065-2717(08)70020-0

[2] Liess, C. (1975). Experimental investigation of film cooling with ejection from a row of holes for the application to gas turbine blades. *Journal of Engineering for Gas Turbines and Power*, 97(1), 21–27. doi: 10.1115/1.3445904

[3] Paradis, M.A. (1977). Film cooling of gas turbine blades: a study of the effect of large temperature differences on film cooling effectiveness. *Journal of Engineering for Gas Turbines and Power*, 99(1), 11–20. doi: 10.1115/1.3446240

[4] Jabbari, M.Y., & Goldstein, R.J. (1978). Adiabatic wall temperature and heat transfer downstream of injection through two rows of holes. *Journal of Engineering for Gas Turbines and Power*, 100(2), 303–307. doi: 10.1115/1.3446350

[5] Azzi, A. & Jubran, B.A. (2007). Numerical modelling of film cooling from converging slot-hole. *Heat and Mass Transfer (Warme und Stoffubertragung)*, 43(4), 381–388. doi: 10.1007/s00231-006-0115-9

[6] Khorsi, A., & Azzi, A. (2010). Computation film cooling from three different holes geometries. *Mechanika*, 86(6), 32–37. doi: 10.5755/j01.mech.86.6.15971

[7] Guangchao, L., Huiren, Z., & Huiming, F. (2008). Influences of hole shape on film cooling characteristics with CO2 injection. *Chinese Journal of Aeronautics*, 21(5), 393–401. doi: 10.1016/s1000-9361(08)60051-5

[8] Liu, C.L., Zhu, H.R., Bai, J.T., & Xu, D.C. (2011). Film cooling performance of converging-slot holes with different exit-entry area ratios. *Journal of Turbomachinery*, 133(1), 1–11. doi: 10.1115/1.4000543

[9] Zaman, K.B.M.Q., Rigby, D.L., & Heidmann, J.D. (2010). Experimental study of an inclined jet-in-cross-flow interacting with a vortex generator. *48th AIAA Aerospace Sciences Meeting Including the New Horizons Forum and Aerospace Exposition*, 4–7 January, Orlando, USA. doi: 10.2514/6.2010-88

[10] Ben Ali Kouchih, F., Boualem, K., & Azzi, A. (2021). Effect of backward injection with combined hole on film cooling performance. *Journal of Mechanical Engineering and Sciences*, 15(3), 8418–8427. doi: 10.15282/jmes.15.3.2021.18.0662

[11] Boualem, K., & Azzi, A. (2020). Blowing Ratio Effect on Film Cooling Performance for a Row Holes Installed in Different Trench Configurations. *Diffusion Foundations*, 28, 65−75. doi: 10.4028/www.scientific.net/DF.28.65

[12] Boualem, K., Bordjane, M., Bourdim, M., Grine, M., Ben Ali Kouchin, F., & Azzi, A. (2023). Numerical investigation of V-shaped trench on film cooling performance. *Thermophysics and Aeromechanics*, 30 (2), 305−315. doi: 10.1134/S0869864323020117

[13] Na, S. & Shih, T.I.-P. (2006). Increasing Adiabatic Film-Cooling Effectiveness by Using an Upstream Ramp. *Heat Transfer, Parts A and B*, 3, 931–938. *ASME Turbo Expo 2006: Power for Land, Sea, and Air*. 8−11 May, Barcelona, Spain. doi: 10.1115/GT2006-91163.

[14] Shinn, A.F., & Pratap Vanka, S. (2013). Large Eddy Simulations of Film-Cooling Flows With a Micro-Ramp Vortex Generator. *Journal of Turbomachinery*, 135(1). doi: 10.1115/1.4006329

[15] An, B., Liu, J., Zhang, C., & Zhou, S. (2013). Film Cooling of Cylindrical Hole With a Downstream Short Crescent-Shaped Block. *Journal of Heat Transfer*, 135(3). doi: 10.1115/1.4007879

[16] Zhou, W., & Hu, H. (2016). Improvements of film cooling effectiveness by using Barchan dune shaped ramps. *International Journal of Heat and Mass Transfer*, 103, 443–456, 2016, doi: 10.1016/j.ijheatmasstransfer.2016.07.066

[17] Zhou, W., & Hu, H. (2017). A novel sand-dune-inspired design for improved film cooling performance. *International Journal of Heat and Mass Transfer*, 110, 908–920. doi: 10.1016/j.ijheatmasstransfer.2017.03.091

[18] Grine, M., Boualem, K., Dellil, A.Z., & Azzi, A. (2020). Improving adiabatic film-cooling effectiveness spanwise and lateral directions by combining BDSR and anti-vortex designs. *Thermophysics and Aeromechanics*, 27(5), 749−758. doi: 10.1134/S0869864320050091

[19] Ben Ali Kouchih, F., Boualem, K., Grine, M., & Azzi, A. (2022). The Effect of an Upstream Ramp On Forward and Backward Injection Hole Film Cooling. *Journal of Heat Transfer*, 142(12). doi: 10.1115/1.4047643

[20] Sinha, A.K., Bogard, D.G., & Crawford, M.E. (1991). Film cooling effectiveness downstream of a single row of holes with variable density ratio. *Journal of Turbomachinery*, 113(3), 442–449. doi: 10.1115/1.2927894

[21] Silieti, M., Divo, E.B., & Kassab, A.J. (2009). The effect of conjugate heat transfer on film cooling effectiveness. *Numerical Heat Transfer, Part B: Fundamentals: An International Journal of Computation and Methodology*, 56(5), 335–350. doi: 10.1080/10407790903508046

[22] El Ayoubi, C., Ghaly, W., & Hassan, I. (2015). Aerothermal shape optimization for a double row of discrete film cooling holes on the suction surface of a turbine vane. *Engineering Optimization*, 47(10), 1384–1404. doi: 10.1080/0305215X.2014.969725

[23] Mayhew, J.E., Baughn, J.W., & Byerley, A.R. (2002). The effect of freestream turbulence on film cooling heat transfer coefficient. Paper GT2002-30173, *ASME Turbo Expo 2002: Power for Land, Sea, and Air*, 3-6 June, Amsterdam, The Netherlands. doi.org/10.1115/GT2002-30173